



HOT WORKABILITY CHARACTERISTICS OF 7075 Al/10% SiCp COMPOSITES

*Rajamuthamil selvan M¹ and Ramanathan S²

^{1,2}Department of Manufacturing Engineering, Annamalai University, Annamalai Nagar, TamilNadu-608002, India

ABSTRACT

An important parameter in the mechanical working of materials is called workability, which is the relative ease with which a metal can be shaped through plastic deformation without the formation of any defect. Workability can be evaluated by means of processing maps, constructed from experimentally generated flow stress variation with respect to strain, strain rate and temperature. The present work is generating processing maps for hot working processes for 7075 Al/10% SiCp composite in the temperature range of 300 to 500 °C and strain rate range of 0.001 to 1 s⁻¹. The processing map exhibits a safe domain of dynamic recrystallization (DRX) with a peak efficiency of power dissipation of about 24% at 400 °C and strain rate of 0.1 s⁻¹. Flow instability occurs due to adiabatic shear bands and flow localizations at higher strain rates above 0.1 s⁻¹ and the corresponding processing conditions are avoided. The safe domains and unsafe domains were validated through microstructural investigations.

Keywords: Hot Working Composites, Processing Map and Dynamic Recrystallization.

1. Introduction

Aluminium (Al)-based metal-matrix composites Reinforcement is added to the matrix of the bulk material to increase strength and stiffness of the matrix. The metal-matrix composites offer a spectrum of advantages that are important for their selection and use as structural materials. A few such advantages include the combination of high strength, high elastic modulus, high toughness, impact resistance, low sensitivity-to changes in temperature or thermal shock, high surface durability, low sensitivity to surface flaws, high electrical and thermal conductivity, minimum exposure to the potential problem of moisture absorption resulting in environmental degradation, and improved fabric ability with conventional metal working equipment [1]. Reinforcements are generally ceramics. Typically these ceramics are oxides, carbides and nitrides, which are used as reinforcements because of their excellent combinations of specific strength and stiffness at both ambient and at elevated temperatures. Silicon carbide, boron carbide and aluminum oxide are the key particulate reinforcements have been used. These can be obtained in varying levels of purity and size distribution. The particulate-reinforced metal-matrix composites have emerged as attractive candidates for use in a spectrum of applications to include industrial, military and space related [1,2].

Workability of a material is specified by its flow stress dependence on processing variables (for example, strain, strain rate, preheat temperature and die

temperature), its failure behavior and the metallurgical transformations that characterize the alloy system to which it belongs. However, the major emphasis in workability is on measurement and prediction of limit of deformation before fracture. One of the requirements for process modeling is knowledge of the material flow behavior for defining deformation maps that delineate 'safe' and 'non safe' hot working conditions. These maps show the processing conditions for stable and unstable deformation in the processing space (that is on axes of temperature and strain rate). The ultimate objective is to manufacture components with controlled microstructure and properties, without macro or microstructural defects, on a repeatable basis in a manufacturing environment [3]. The input to generate a processing map is the experimental data of flow stress (σ) as a function of temperature (T), strain rate ($\dot{\epsilon}$) and strain (ϵ). As the map generated will be only as good as the input data. It is important to use the accurate, reliable and yet simple experimental technique for generating them. While hot tensile, hot torsion or hot compression techniques may be used for this purpose, hot compression test has decisive advantages over others. By conducting compression test on a cylindrical specimen, it is easy to obtain a constant true strain rate using an exponential decay of the cross-head speed and to conduct the test under isothermal conditions [4]. In hot forming of metals at temperatures above recrystallization temperature, the influence of strain on

*Corresponding Author - E-mail: rajanarmi@yahoo.co.in

flow stress is insignificant and the influence of strain rate (i.e. rate of deformation) becomes increasingly important. Conversely, at room temperature (i.e. in cold forming), the effect of strain rate on flow stress is negligible and the effect of strain on flow stress (i.e. strain hardening) is most important. The degree of dependency of flow stress on temperature varies considerably among different materials. Therefore, temperature variations in a forming operation can have quite different effects on load requirements and on metal flow for different materials. Bulk metal working processes, such as rolling, forging and extrusion are performed on a variety of machines. The strain rates achievable depend on the speed of the machine, the geometry of the deformation zone and the geometry of the work piece. To define the processing windows in the desired range of strain rates, workability parameters should be optimum in the specified temperature domain.

G. Ganesan et al [5] have developed processing map on 6061 Al –10 vol % SiC particulate composite. In their dynamic materials model, the work piece under hot working conditions is considered to be a dissipator of power. The variation of a dimensionless parameter (η) called the efficiency of power dissipation, with strain (ϵ), strain rate ($\dot{\epsilon}$) and temperature (T) constitutes a processing map. They computed the efficiency of power dissipation (η) defined in Refs. [3, 5-8] in terms of the strain rate sensitivity parameter (m) as,

$$\eta = 2m/m+1 \quad (1)$$

For the identification of flow instabilities during hot deformation of materials, they utilized the following condition proposed in Refs. [3, 5-8]:

$$\xi(\dot{\epsilon}) = \frac{\delta \ln(m/m+1)}{\delta \ln \dot{\epsilon}} + m < 0 \quad (2)$$

In fact, the efficiency of power dissipation (η) given in Eq. (1) explicitly in terms of the strain rate sensitivity parameter (m), is valid only when the flow stress (σ)–strain rate ($\dot{\epsilon}$) curve obeys power law [3, 8]:

$$\sigma = K\dot{\epsilon}^m \quad (3)$$

For this case, the parameter, m is independent of $\dot{\epsilon}$ and the flow instability condition given by Eq. (2) reduces to $m < 0$. For complicated alloy systems, the flow stress with respect to $\dot{\epsilon}$ does not obey power law and the computation of η in terms of m from Eq. (1) and the flow instability condition given in Eq. (2) become erroneous. That means that Eq. (2) in both cases is meaningless. In the present paper, the hot compressive

behavior of 7075 Al/10% SiCp composite was examined by compressive tests. The processing maps were constructed on the basis of the variations of power dissipation efficiency and instability parameters with temperature and strain rate. Subsequently identify various microstructural mechanisms and domains of safe and unsafe regions through microstructure observations. The optimum workability was designed by the processing maps.

2. Experimental Studies

Stir casting technique was used to fabricate 7075Al alloy reinforced with 10% volume fraction of silicon carbide Composites. The matrix material was 7075 Aluminium Alloy (Composition in wt% Cu 1.66, Mg 2.10, Si 0.14, Mn 0.21, Fe 0.40, Cr 0.18, Zn 5.67, Ti 0.01 and rest Al) and the reinforcement was SiC_p with average size of 5 μ m. The aluminium alloy was melted by using an Electric Furnace. Preheated SiC_p (250°C) was added to the melt and mixed by using a rotating impeller in Argon environment and poured in permanent mould. The cast billets were soaked in the temperature of 400°C for 30 minutes and hot extruded. The cylindrical specimens of dimensions, 10 mm in diameter and 10 mm in Height were machined from the extruded rods.

The hot compression tests [4] were performed on a 10T servo controlled universal testing machine for different strains (0.1 – 0.5), strain rates (0.001s⁻¹ to 1.0s⁻¹) and temperatures (300 to 500°C). Temperature of the specimen was monitored with the aid of a chromel/alumel thermocouple embedded in a 0.5mm hole drilled half the height of the specimen as stated by O.Siva [9] and Prasad Y.V.R.K. et al [10]. The thermocouple was also used for measuring the adiabatic temperature rise in the specimen during deformation. The specimens were effectively lubricated with graphite and deformed to a true strain of 0.5. After compression testing, the specimens were immediately quenched in water and the cross section was examined for microstructure. Specimens were deformed to half of the original height. Deformed specimens were sectioned parallel to the compression axis and the cut surface was prepared for metallographic examination. Specimens were etched with Keller's solution. The microstructure of the specimens was obtained through Versamet 2.0 optical microscope with Clemex vision Image Analyser and mechanism of deformation was studied. Using the flow stress data, power dissipation efficiency and flow instability were evaluated for different strain rates, temperatures at a constant strain of 0.5. The processing map was developed for 0.5 strains for 7075Al/10% SiC_p composites.

3. Method of Analysis

The mechanical behavior of materials under processing is generally characterized by the constitutive equations which relate the flow stress (σ) to the strain (ϵ), strain rate ($\dot{\epsilon}$) and temperature (T). S.V.S. Narayana Murty and co-workers [3,5-8] have developed processing maps on the basis of the principles of dynamic materials model (DMM). According to the DMM, the power, P (per unit volume) absorbed by the work piece material during plastic flow is given by,

$$P=G+J \quad (4)$$

or

$$\sigma \dot{\epsilon} = \int_0^{\epsilon} \sigma d\epsilon + \int_0^{\sigma} \dot{\epsilon} d\sigma \quad (5)$$

The G term represents the power dissipated by plastic work, most of which is converted into viscoplastic heat; the little remaining power is stored as lattice defects. The dissipator power co-content J is related to the metallurgical mechanisms, which occur dynamically to dissipate power. In the variation procedure, the G content is the work function and the J co-content is a complementary set. From Eq. (5), it follows that at any given (ϵ) and T, the change in J with respect to G yields the well known strain rate sensitivity parameter (m), which is,

$$m = \frac{\partial \log \sigma}{\partial \log \dot{\epsilon}} \Big|_{\epsilon, T} = \left(\frac{\sigma J}{\sigma G} \right)_{\epsilon, T} \quad (6)$$

The value of J at a given strain (ϵ), strain rate ($\dot{\epsilon}$) and temperature (T) is estimated from the measured flow stress (σ) data. Though the definition of the strain rate sensitivity parameter (m) in Eq. (6) originates directly from the traditional power law relation (3), when the log-log data from the σ - $\dot{\epsilon}$ plot does not fall on a straight line, m the slope of the $\log \sigma$ - $\log \dot{\epsilon}$ curve varies at each and every point on the curve, and becomes a function of $\dot{\epsilon}$. At low strain rates, the $\log \sigma$ - $\log \dot{\epsilon}$ plot represents a straight line, for which the slope, m is a constant. Hence, the apparent m values from Eq. (6) depend on deformation mechanisms in the region for given strain rates and temperatures. If the flow stress obeys power law (3) as assumed in Refs. [2-5], then the dissipator content (G) and the dissipator co content (J) can be obtained directly from the two integrals in Eq. (5) as

$$G = P / (1 + m) \quad (7)$$

$$J = m P / (1 + m) \quad (8)$$

These can be evaluated directly from P and m. For ideally plastic flow, the flow stress is proportional to the strain rate at any strain and temperature ($m=1$). For this case the value of J becomes,

$$J_{max} = 1/2 P \quad (9)$$

The behavior of super plastic materials approaches this extreme. The other extreme occurs for materials which are strain rate insensitive, i.e, $m \rightarrow 0$ or $J = 0$. When $J=0$, $G= P$ and all the power would be dissipated by heat which leads to plastic instability by a continuum process such as adiabatic shearing. The metallurgical dissipation processes may be characterized by the variation of J co-content with strain, temperature and strain rate, but normalization with input power (P) sharpens the variation. Thus comparison with a linear ideal dissipator ($m=1$) in which maximum possible dissipation through J co content (Eq. (9)), leads to the definition of a dimensionless parameter, η given by:

$$\eta = J / J_{max} = 2J/P \quad (10)$$

Substituting the value of J from Eq. (8) in Eq. (10), one can obtain the value of η explicitly in terms of m as given in Eq. (1) which is valid for the flow stress at any strain and temperature obeying the power law as in Eq. (3).

4. Results and Discussion

The flow stress data was generated covering the temperature range of 300 to 500°C and strain rate range 0.001 to 1.0 s⁻¹ from compression testing of solid cylinders of size 10mm in diameter and 10 mm in height using servo hydraulic testing machine which is capable of imposing constant true strain rates on the specimen. Adiabatic temperature rise during high strain rate testing was measured and the flow stress was corrected for the temperature rise. The specimens were compressed to 50% of their initial height and the load-stroke curves obtained in the hot compression were converted in to true stress-true plastic strain curves by subtracting the elastic portion of the strain and using the standard equations for the true stress and true strain calculations. The values of the efficiency parameter (η) and the strain rate sensitivity parameter (m) [11] are determined from the flow stress data of the material.

4.1 Flow behavior

The flow stress behaviour of metal matrix composites is governed by two main processes: the

transfer of load from the ductile matrix to the hard particles and the microstructural transformations such as recrystallization or damage phenomena; in this case the material can present decohesion at the interfaces matrix–particles or several particle cracking. When the material is able to dissipate the provided power through the load transfer or through metallurgical transformations it does not reach high levels of damage [12, 13].

The flow stress–true strain curves obtained on specimens deformed at different temperatures and strain rates. Basically, these revealed that the flow stress increased rapidly before softening occurred and flow softening is significant at lower temperatures and higher strain rates. The curves tend to exhibit steady state flow at lower strain rates and higher temperatures. When dynamic recrystallization entirely balances strain hardening, a steady state in the stress–strain curve is observed. This means that there is no net storage of energy occurring. In this stage the area of the curve on the stress axis is zero. At high strain rates when the rate of strain hardening is high, the co-content area has to be correspondingly higher. Enhanced dynamic recrystallization at higher temperatures, on the other hand, tends to ‘bend’ the curve downward. This decreases the co-content area. As deformation proceeds, the incremental co-content area decreases implying that dynamic recrystallization is progressively reducing the efficiency of energy storage affected by strain hardening an investigation into the nature of DRX might be possible through a study of the evolution of the stored energy. But, it has been proposed that in addition to the attainment of a critical level of stored energy, a critical rate of energy dissipation must also be achieved in order for DRX to commence [14].

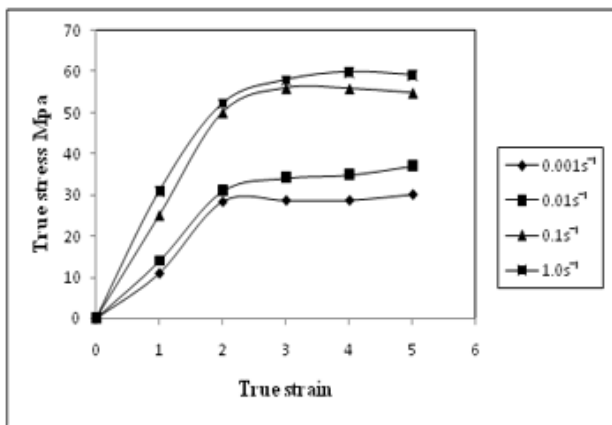


Fig. 1 The Flow Curves for Different Strain Rates at Constant Temperature of 400°C

Flow curves obtained for Al/10% SiC_p composites deformed in compression at 400°C at different strain rates ranging from 0.001 to 1.0 s⁻¹ are shown in Fig 1. The typical characteristics are as follows:

- (i) At lower strain rates, oscillations are observed in the flow stress. The oscillations are not readily apparent since the noise in the data sometimes proved to be of larger amplitude than the oscillations themselves.
- (ii) The strain corresponding to the peak in flow stress increases with increase in strain rate and decrease in temperature.

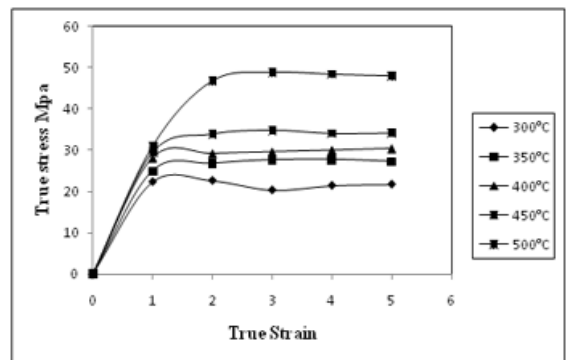


Fig. 2 The Flow Curves for Different Temperatures at Constant Strain Rate of 0.1s⁻¹

The flow curves for different temperatures at constant strain rate 0.1s⁻¹ are shown in Fig 2. The flow curves obtained at high temperatures show a peak in the flow stress followed by softening to a steady state. (It will be seen later that the peak is exhibited at all conditions but at higher strains.) High rate of dislocation annihilation associated with rapid thermal softening occurs with the high temperature regimes [15]. The stress–strain curves exhibited flow softening at all strain rates when tested at 300°C, while at temperatures above 400°C and at strain rates lower than 0.1 s⁻¹ the flow curves reached a steady state. According to them the matrix around the reinforcement particles presents higher dislocation density regions. These high dislocation density regions restrict the plastic flow and contribute to the strengthening mechanism resulting in higher strain hardening. As the temperature increases, the strengthening effect of reinforcement particles is considerably diminished, so that the material shows softening behaviour at higher temperature. The occurrence of dynamic recrystallization (DRX) at higher temperature and higher strain rates, deformation leads to a significant reduction in flow stress in this deformation ranges [16].

4.2 Processing map

A superimposition of the instability map on the power dissipation map gives a processing map which reveals domains (efficiency contours converging towards a peak efficiency) where individual microstructural processes occur and the limiting conditions for the regimes (bounded by a contour for $\xi = 0$) of flow instability [2]. Processing maps help in identifying temperature – strain rate windows for hot working where the intrinsic workability of the material is maximum (e.g. dynamic recrystallization (DRX) or super plasticity) and also in avoiding the regimes of flow instabilities (e.g. adiabatic shear bands or flow localization). The processing map technique has been used earlier to study the hot deformation mechanisms in Al alloys [8, 13, 17] including dynamic recrystallization (DRX) and flow instabilities.

The processing map at a strain of 0.5 is shown in Fig 3. This strain may be considered large enough to represent steady state flow. The map exhibits single domain, it occurring in the temperature range of 355 to 410°C. The domain occurs in the lower strain rate range (0.014 to 0.18 s⁻¹) with a peak efficiency of about 24% occurring at 400°C and 0.1 s⁻¹.

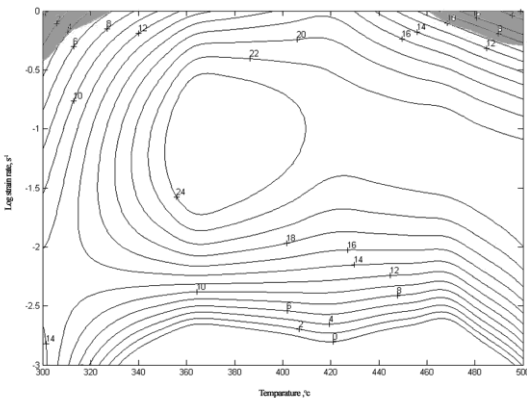


Fig. 3 Processing Map for 7075Al/10% SiCp Composites at 0.5 Strain

According to the instability criterion (Eq. (2)), a large domain of flow instability at higher strain rates above about 0.1 s⁻¹ is shown in shaded area of Fig. 3. The Aluminium alloy exhibits the unstable domain at higher strain rates due to the occurrences of adiabatic shear bands or localized plastic flow. As shown in Figure 3, the domains with similar efficiency of power dissipation might correspond to different deformation mechanisms. Therefore, these domains require further validation by Microstructure analysis.

4.3 Microstructure analysis

4.3.1 Stability zones

Dynamic recrystallization (DRX) is a beneficial process in hot deformation as it gives the simultaneous occurrence of dynamic restoration processes and helps to soften the material and the recovery mechanisms leading to DRX are likely to be strain rate dependent. Therefore, DRX is a chosen domain for hot workability optimizing and good microstructural control [18]. Microstructure analysis reveal that the initial microstructures have been replaced (Figure 4) by recrystallized structure. Based on these observations, this domain represents the region of possible dynamic recrystallization. DRX is a beneficial process in hot deformation since it gives stable flow and good workability to the materials by simultaneously softening. However, it reconstitutes the microstructure.

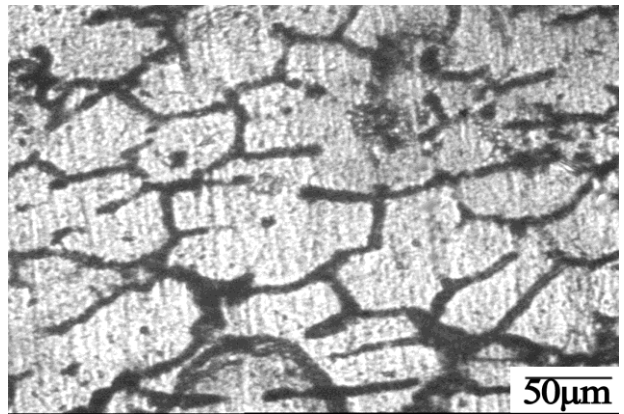


Fig. 4 Dynamic Recrystallization at 400°C at a Strain Rate of 0.1s⁻¹

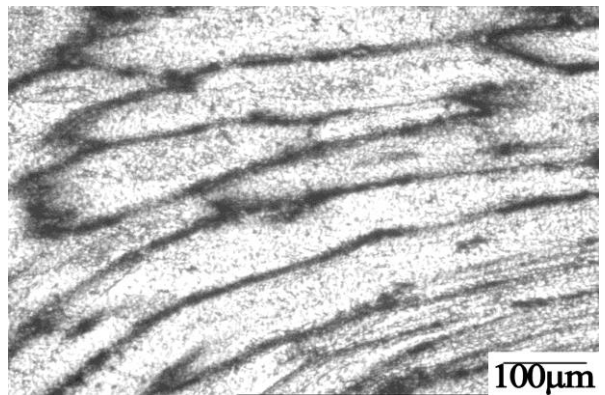


Fig. 5 Grain Elongation at 400°C and at a Strain Rate of 0.01s⁻¹

It is noticed that the range from 355°C to 410°C is the DRX domain and it is safe domain for bulk metal process. DRX observed at the temperature 400°C and a strain rate of 0.1 s⁻¹ is the optimum range for bulk metal working in the safe domain as obtained from the power dissipation map which is shown in the Fig 4. Thus, power dissipation map obtained can help in optimizing the process. Grain elongation is observed at the temperature of 400°C at strain rate 0.1s⁻¹ which is shown in Fig 5.

4.3.2 Instability zones

At higher strain rates, the deformation is adiabatic. Heat generated during hot working is not conducted away due to insufficient time and low thermal conductivity, inducing highly localized flow along the maximum shear stress plane [19]. Fig. 6 shows micrograph of the specimens deformed at the temperature of 300°C and strain rate of 1.0 s⁻¹, where adiabatic shear bands can be observed at an angle of about 45° to the compressive axis. Therefore, flow instability below 355°C and strain rate of 1.0 s⁻¹ is induced by the adiabatic shear bands as shown in Figure 6.

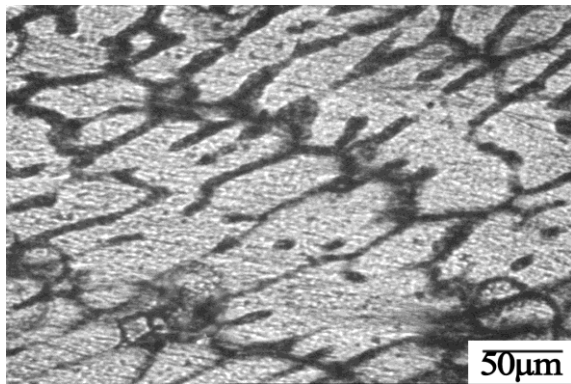


Fig. 6 Shear Band Formation at 300°C and at a Strain Rate of 1.0s⁻¹

The transfer of load from the ductile matrix to the hard particles and the microstructural transformations such as recrystallization or damage phenomena; in this case the material can present decohesion at the interfaces matrix–particles or several particle cracking. When the material is able to dissipate the provided power through the load transfer or through metallurgical transformations, it does not reach high levels of damage [12, 13]. Voids formation is observed at 300°C and 1.0 s⁻¹ which is shown in Fig 7. The structure is characterized by big voids formation (occurs at lower temperatures and high strain rates) at the inter

phase particles-matrix and by the presence of many fractured particle in particular at 350°C.

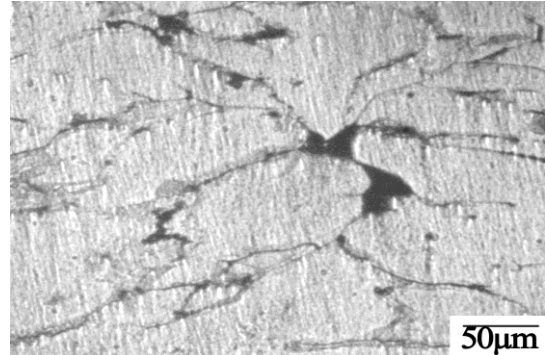


Fig. 7 Voids Formation at 500°C and at a Strain Rate of 1.0s⁻¹

The flow localization is due to the cracking of silicon particle and adiabatic shear bands present in the metal matrix, which are the manifestations of flow instability predicted by the instability map.

Hard particles are present in a soft matrix, deformation causes the interface to crack and deboned since the matrix undergoes plastic flow while the particles do not deform. The interfacial failure observed in the current composites is also different from the simple interfacial debonding that the SiC particles are pulled out from metal matrix with clear surfaces [20]. These differences might be explained by the high strength of metal matrix and SiC/Al interfaces in the composites produced in the current experiment. The Fig 8. shows that the Debonding between the particles and the matrix is weak. It is evident that the particle deboning is due to interfacial failure. Aluminium matrix is seen sticking to the surface of the SiC particle. A gap between the matrix and the particle is also seen. The feature is observed at 450 °C in 1.0 s⁻¹.

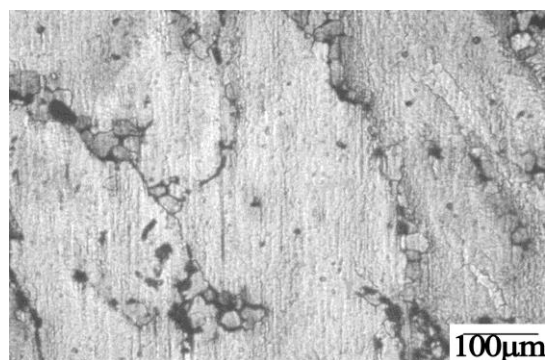


Fig. 8 Debonding at 300°C and at a Strain Rate of 1.0s⁻¹

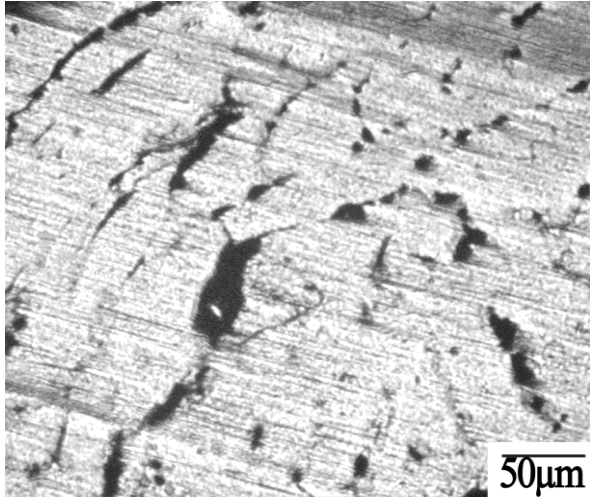


Fig. 9 Matrix Cracking at 500°C and a Strain Rate of 1.0s⁻¹.

Two processes mainly govern the flow response of particle-reinforced metal matrix composites; the first involves load transfer from the matrix to the particles, leading to an increase in flow-stress. The second process involves the development of microstructural damage, usually in the form of particle cracking or de-cohesion of the particle–matrix interface [12]. These processes are not independent, but are strictly related to each other; for example, particle cracking occurs when hard particles are subjected to a very high stress, i.e. when high loads are transferred from the soft matrix to the reinforcements. This process, in turn, is possible only when the interface between particles and matrix is largely undamaged. Fig. 9 shows matrix cracking at 500°C and a strain rate of 1.0s⁻¹.

5. Conclusions

The hot deformation behavior of 7075 Al/10% SiCp metal matrix composite was investigated with compression tests in the temperatures and strain rate ranges of 300 – 500°C and 0.001-1.0s⁻¹, respectively. The processing map was constructed on the basis of the variations of power dissipation efficiency and instability parameters with temperature and strain rate. The optical microscopy observations used to identify the metallurgical transformations.

The safe domain occurs in the strain rate range (0.014 – 0.18 s⁻¹) with a peak efficiency of about 24 % occurring at 400°C and 0.1 s⁻¹. The unsafe domain occurs at higher strain rate of 1.0 s⁻¹ and at the temperature ranges of 300 – 350 °C and 450 – 500 °C which are to be avoided during processing.

References

1. Ali Kalkanl and Sencer Yilmaz (2008), "Synthesis and Characterization of Aluminum Alloy 7075 Reinforced with Silicon Carbide Particulates", *Material Design*, Vol.29, 775–780.
2. Lee Kon Bae and Kwon Hoon (2002), "Strength of Al–Zn–Mg–Cu matrix Composite Reinforced with SiC Particles", *Metall. Mater. Trans. A*, Vol. 33, 455–465.
3. Narayana Murty S V S, Nageswara Rao B and Kashyap B P (2005), "Identification of Flow Instabilities in the Processing maps of AISI 304 Stainless Steel", *Journal of Material Processing Technology*, Vol. 166, 268–278.
4. Lin Y C, Ming-Song Chen and Jue Zhon (2008), "Prediction of 42CrMo Steel Flowstress at High Temperature and Strain Rate", *Mech. Res. Commun.*, Vol. 35(3), 142–150.
5. Ganesan G, Raghukandan K, Karthikeyan R and Pai B C, (2005), "Development of Processing Map for 6061 Al/15% SiCp Composites Through Neural Networks", *Journal of Material Processing Technology*, Vol. 166,423–429.
6. Rao K P, Prasad Y V R K, Hort N and Kainer K U (2008), "Hot Workability Characteristics of Cast and Homogenized Mg–3Sn–1Ca Alloy", *Journal of Material Processing Technology*, Vol. 201, 359–363.
7. Prasad Y V R K and Rao K P (2009), "Effect of Homogenization on the Hot Deformation Behavior of Cast AZ31 Magnesium Alloy", *Material Design*, Vol. 30, 723–730.
8. Narayana Murty S V S, Nageswara Rao B and Kash B P (2005), "On the Hot Working Characteristics of 2014 Al–20 vol% Al₂O₃ Metal Matrix Composite", *Journal of Material Processing Technology*, Vol.166, 279–285.
9. Siva and Prasad O (2002), "Characteristics of Super Plasticity Domain in the Processing Map for Hot Working of as Cast Mg–11.5 Li–1.5 Al Alloy", *Material Science and Engineering A*, Vol. 323,270-277.
10. Prasad Y V R K and Rao K P (2005), "Processing Maps and Rate Controlling Mechanisms of Hot Deformation of Electrolytic Tough Pitch Copper in the Temperature Range 300-950°C", *Material Science and Engineering A*, Vol. 391, 141–150.
11. Seshacharyulu T, Medeiros S C, Morgan J T, Malas J C, Frazier W G and Prasad Y V R K (2000), "Hot Deformation and Microstructural Damage Mechanisms in Extra Low Interstitial (ELI) grade Ti-6Al- 4V", *Material Science and Engineering*, Vol. 279, 289–299.
12. Spigarelli S, Cerri E, Cavaliere P and Evangelista E (2002), "An Analysis of Hot Formability of the 6061+20% Al₂O₃ Composite by Means of Different Stability Criteria", *Material Science and Engineering A*, Vol. 327, 144–154.
13. Cavaliere P, Cerri E and Leo P (2004), "Hot Deformation and Processing Maps of a Particulate Reinforced 2618/Al₂O₃/20p Metal Matrix Composite", *Composites Science and Technology*, Vol. 64, 1287–1291.
14. Rao K P, Ramkumar and Oruganti K (2003), "Study of Hot Deformation Through Energy Storage Concept", *Journal of Material Processing Technology*, Vol. 138, 97–101.

15. Woei-Shyan Lee, Chi-Feng Lin and Sen-Tay Chang (2000), "Plastic Flow of Tungsten-Based Composite Under Hot Compression", *Journal of Material Processing Technology*, Vol. 100, 123–130.
16. Raghunath B K, Karthikeyan R, Ganesan G and Gupta M (2008), "An Investigation of Hot Deformation Response of Particulate-Reinforced Magnesium + 9% Titanium Composite", *Material Design*, Vol. 29, 622–627.
17. Radhakrishna Bhat B V, Mahajan Y R, Roshan H Md and Prasad Y V R K (1995), "Processing Map for Hot Workability of 6061–10 vol% Al₂O₃ Metal Matrix Composite", *Material Science and Technology*, Vol. 11, 167–173.
18. Li A B, Huang L J, Meng Q Y, Geng L and Cui X .P (2009), "Hot working of Ti–6Al– 3Mo–2Zr–0.3Si Alloy with Lamellar $\alpha+\beta$ Starting Structure Using Processing Map", *Mater. Design*, Vol.30, 1625–1631.
19. Zeng W D, Zhou Y G, Zhou J, Yu H Q, Zhang X M and Xu B (2006), "Recent Development of Processing Map Theory", *Rare. Metal. Mater. Eng.*, Vol.35, 673–677.
20. Nie S H and Basaran C A (2005), "A Micromechanical Model For Effective Elastic Properties of Particulate Composites With Imperfect Interfacial Bonds", *Int. J. Solids Struct.* Vol. 42, 4179–4191.

Acknowledgement

The authors are grateful to the Department of Manufacturing Engineering, Annamalai University, Tamilnadu, India for the support rendered for the fabrication and testing of Composites.